# PERFORMANCE OF MECHANICAL FACE SEALS WITH SURFACE MICROPORES

**M. Mahbubur Razzaque and M. Tanvir Rahman Faisal**
Department of Mechanical Engineering
Bangladesh University of Engineering and Technology
(BUET), Dhaka-1000, Bangladesh

## INTRODUCTION

The attempt to improve the performance of machine elements through modification of surface texture is very old. One of the early works by Salama[1] studied the effect of macroroughness on the performance of parallel thrust bearings. Similar studies with wavy mechanical seals were carried out by Pape[2] and Etsion[3]. Hamilton et al.[4] did some wonderful experiments with surface microasperities. Based on these experiments, a theoretical model was developed by Anno et al.[5] assuming small tilts on asperity tops. In a following work[6] they compared the load support and the leakage performance of positive and negative asperities using the small tilt model. Sneak[7-8] showed in an investigation that misalignment and surface waviness affect face seal performance in the same order the change in clearance affects the performance of the aligned seal surfaces. Lai[9] showed that grooves of small depth may keep the parallel faces apart. Etsion and Burstein[10] developed a mathematical model for a face seal with hemispherical pore arranged in a rectangular array on its surface. Subsequently, Etsion et al.[11-12] presented experimental results with laser textured seal faces and demonstrated the enhancement of the life of a face seal. Now-a-days, with different micro-machining techniques, it is possible to produce microstructures of any shape. It is, therefore, essential to study the possibility of using non-hemispherical micropores to improve the face seal performance.

Recently, Faisal[13] and Faisal and Razzaque[14] developed a mathematical model for face seals with micropores of arbitrary shape. This paper reports the result of a parametric study applying the model to face seals with exponential pores. The seal performance parameters such as equilibrium seal clearance, friction torque and leakage across the seal are calculated and presented for a range of sealed pressure, pore size and pore ratio of the annular surface area. Using microstructures in the form of elliptical pores improves the seal performance up to a pore ratio of 15%. Increasing the pore ratio beyond this, improvement of the seal performance is very negligible. The optimum pore size depends on the sealed pressure and a critical pore size exists at which seal failure may occur.

## PHYSICAL MODEL

Along the plane of the annular seal surface circular pores are arranged in rectangular arrays and each pore has a radius of $R_o$. In a plane perpendicular to the seal surface, the pore section is exponential with a pore depth of $h_p$ at its center, as shown in Fig. 1(a). The pores are evenly distributed with an area ratio, $S$. The distance between neighboring pores, $2R_1$, is assumed to be large enough so that the interaction among the pores is negligible. Each pore is located at the center of an imaginary "control cell"

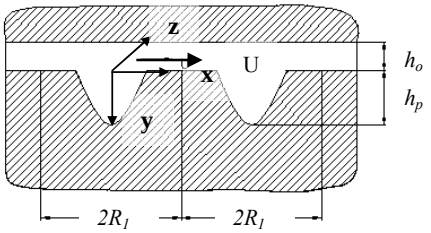


Figure 1(a): Cross section of the pores.

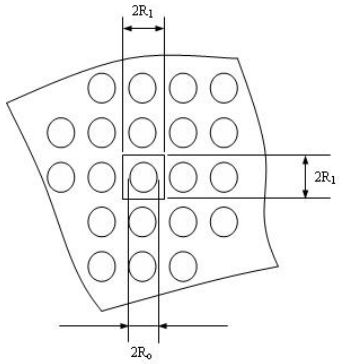


Figure 1(b): Control cell with coordinate system.

of sides $2R_1 \times 2R_1$, as shown in Fig. 1(b). It is assumed that the sealed fluid is Newtonian and a fluid film of constant thickness $h_o$ is maintained between the parallel surfaces of the seal. The hydrodynamic pressure distribution over each control cell is exactly the same. Hydrostatic pressure drops linearly from seal's outer to inner boundary.

## MATHEMATICAL MODEL

Using the nondimensional parameters $X = \frac{x}{R_0}, Z = \frac{z}{R_0}$, $H = \frac{h}{h_0}$, $\xi = \frac{R_1}{R_0}$, $\psi = \frac{h_p}{h_0}$, $P = \frac{p}{\Lambda}$ and $\Lambda = \frac{6U\mu R_0}{h_0^2}$, the famous Reynolds equation for the hydrodynamic pressure distribution in region $2R_1 \times 2R_1$ of a control cell may be expressed as,

$$\frac{\partial}{\partial X}\left(H^3 \frac{\partial P}{\partial X}\right) + \frac{\partial}{\partial Z}\left(H^3 \frac{\partial P}{\partial Z}\right) = \frac{\partial H}{\partial X} \qquad (1)$$

where, $H = 1$ for outside the pore and $H = Ae^{B\rho}$ for over the pore. Here, $\rho = R/R_0$ is the dimensionless radial coordinate over the pore (i.e., $0 \le \rho \le 1$), $A = 1 + \Psi$ and $B = -\ln A$. The dimensionless boundary conditions are: $P = 0$ *at* $X = \pm\xi$ and $Z = \pm\xi$. If the pore size is S portion of a control cell of size $2R_1 \times 2R_1$, $\xi = 0.5(\pi/S)^{0.5}$.

## SOLUTION PROCEDURE AND CALCULATION

The system of linear equations obtained by discretizing Eq. (1) using finite difference technique is solved by successive over relaxation method to get the hydrodynamic pressure components at various grid points of a control cell. Total dimensionless local pressure at each control cell is $P_t = P + P_s$. Here, the dimensionless local hydrostatic pressure $P_s$ is estimated by the following equation based on the assumption of linear hydrostatic pressure drops from the seal outer to inner boundary.

$$p_s = p_i + (p_o - p_i)(r - r_i)/(r_o - r_i) \qquad (2)$$

where, $p_i$ and $p_o$ are the hydrostatic pressures at the seal inner and outer radii, respectively. The dimensionless local hydrostatic pressure is defined as $P_s = p_s/\Lambda$. The hydrodynamic pressure $P$ is made zero according to the half-sommerfeld condition at each point of a cavitating control cell. The hydrodynamic load per unit area of the n-th control cell can be calculated from

$$\overline{W_n} = \int_{-\xi}^{\xi}\int_{-\xi}^{\xi} PdXdZ \qquad (3)$$

Equation (3) is evaluated numerically using Simpson's 1/3rd rule and the dimensional load support over the n-th cell is given by, $W_n = \overline{W_n}\,\Lambda\, R_0^2$ . The total opening force tending to separate the seal ring is,

$$W = \pi\left(r_0^2 - r_i^2\right)\left(p_0 - p_i\right) + \sum_{n=1}^{N_c} W_n$$

This opening force is balanced by a closing force $F_c$, given by $F_c = \pi(r_o^2 - r_i^2)[p_f + B_r(p_o - p_i)]$ and an equilibrium seal clearance is established. Here, $p_f$ is spring force used to close the seal clearance and $B_r$ is balance ratio, which is usually less than unity for a highly pressurized seal. To find the seal clearance, a certain clearance is assumed and the corresponding opening force $W$ is calculated and compared with the closing force $F_c$. The whole procedure is repeated with a different value of seal clearance until the balance is achieved. Neglecting the effect of pressure gradient, the total friction over the annular sealing area, A can be written as,

$$F = \int_{nonpore\ \ area} \mu\frac{U}{h}dA + \int_{pore\ \ area} \mu\frac{U}{h}dA$$

The first integral can be written in terms of pore ratio, $S$ as,

$$\int_{nonpore\ \ area} \mu\frac{U}{h}dA = \pi\mu U\frac{\left(r_o^2 - r_i^2\right)(1-S)}{h_0}$$

The second integral can be rearranged in terms of pore ratio, $S$, as,

$$\int_{pore\ area} \mu\frac{U}{h}dA = \frac{2\pi\mu US\left(r_0^2 - r_i^2\right)}{h_0} \times \frac{[1 - A(B+1)]}{AB^2}$$

Then the friction force can be obtained from the above three equations as,

$$F = \pi\mu U\left(r_0^2 - r_i^2\right)\left[\frac{1-S}{h_0} + \frac{2S}{h_0} \times \left\{\frac{1-(1+\psi)\left[1-ln(1+\psi)\right]}{(1+\psi)\left[-ln(1+\psi)\right]^2}\right\}\right]$$

The dimensionless friction force may then be written as,

$$\overline{F} = \frac{F.h_p}{\pi\mu U\left(r_0^2 - r_i^2\right)} = (1-S)\psi + 2S\psi\left\{\frac{1-(1+\psi)\left[1-ln(1+\psi)\right]}{(1+\psi)\left[-ln(1+\psi)\right]^2}\right\}$$

So, the friction torque of the seal is $T = Fr_m$, where, $r_m = (r_o + r_i)/2$. Based on Poiseuille's law the leakage across the seal is given by,

$$Q = \frac{\pi h_o^3 r_m}{6\mu}\frac{p_o - p_i}{r_o - r_i}$$

**RESULTS AND DISCUSSION**

Different input parameters used for evaluating seal performance in this analysis are listed below:

| **Parameter** | **Numerical Value** |
|---|---|
| Seal inside radius, $r_i$ | 28.4 mm |
| Seal outer radius, $r_o$ | 31.1 mm |
| Spring pressure, $p_f$ | 0.415 MPa |
| Balance ratio, $B_r$ | 0.79 |
| Mean sliding velocity, $U$ | 9.5 m/s |
| Viscosity, $\mu$ | 25 m. Pa-s |
| Friction coefficient | 0.1 |

The sealed pressure was varied from 0.5 MPa to 3.0 MPa. The iterative procedure seeking the balance between the opening force and the closing force was terminated when the seal clearance became smaller than an arbitrary limiting gap of 0.01μm. Different pore ratios such as 2.5%, 11.25%, 15% and 20% are considered for the evaluation of the seal performance.

Figure 2 shows the effect of pore size and pore ratio on seal clearance when the sealed pressure varies from 0.5 to 3 MPa. Pore size is given as the diameter of the pore, $R_o$, in the sliding plane and the pore ratio is defined as the ratio of the area covered by the pores to the total seal area expressed in percentage. It is evident from the figure that at a small sealed pressure, there exists an optimum pore size for which the seal clearance is the maximum. For example, at a pore ratio of 2.5% and a sealed pressure of 0.5 MPa, the optimum pore diameter is about 15 μm at which the seal clearance is the maximum and is about 5.4 μm. After this point, the seal clearance decreases rapidly. As the sealed pressure increases, the seal clearance as well as the optimum pore size decreases. Similar behavior of seal clearance and pore size is found also for pore ratio of 20%. For the sealed pressure of 0.5 MPa, the maximum seal clearance is about 7.4 μm and the optimum pore diameter is 22 μm. Thus an increase in the pore ratio increases both the maximum seal clearance and the optimum pore diameter. For any sealed pressure, there exists a pore diameter for which the seal clearance ceases to exist. This

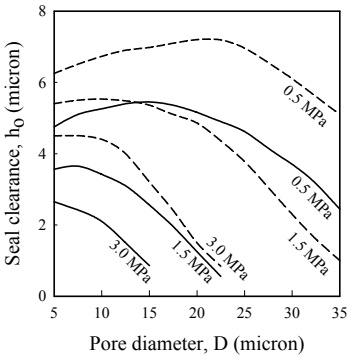


Figure 2: Effect of pore diameter and sealed pressure on seal clearance. The solid lines are for 2.5% pore ratio and the broken lines are for 20% pore ratio. The accompanying labels indicate sealed pressure.

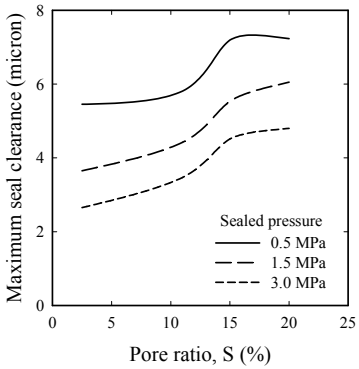


Figure 3: Effect of pore ratio on the maximum seal clearance at different sealed pressures.

pore diameter is very critical for the life of a seal and must be avoided. The pores on a seal surface, therefore, should not be bigger than the optimum diameter at its sealed pressure.

Figure 3 shows the effect of pore ratio on the maximum seal clearance for the same range of sealed pressure. It is clearly visible that irrespective of sealed pressure, the seal clearance increases with the increase of pore ratio. But, as the number of pores on the sealing area increases, the effect of cavitation becomes more prominent and consequently the hydrodynamic load support also increases. When the number of pores exceeds a threshold, the probability of interactions among them increases and the distinction between converging and diverging area diminishes. This leads to hydrodynamic effect lower than that expected without interactions among the pores. As a result, the rate of increment of the seal clearance with the increase of pore ratio slows down as the pore ratio goes beyond 15%.

The relationship between the friction torque and the pore diameter for various sealed pressures between 0.5 ~ 3.0 MPa is shown in Fig. 4. It is evident that the friction torque is the lowest at the point of the optimum pore diameter and that is the point of the maximum seal clearance. At a given sealed pressure, the magnitude of the friction torque remains almost the same for all pore diameters below the optimum pore diameter. Beyond the optimum pore diameter the friction torque increases significantly. It is interesting to note that at large pressures,

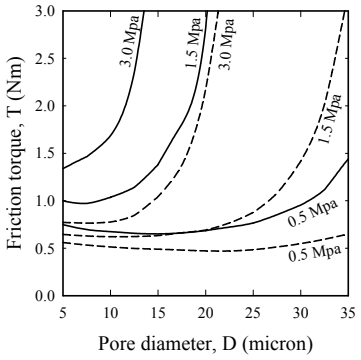


Figure 4: Effect of pore diameter on friction torque at different sealed pressures. The solid lines are for 2.5% pore ratio and the broken lines are for 20% pore ratio.

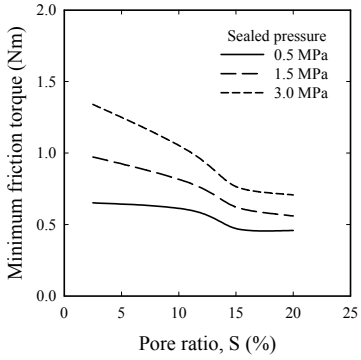


Figure 5: Effect of pore ratio on the minimum friction torque at different sealed pressures.

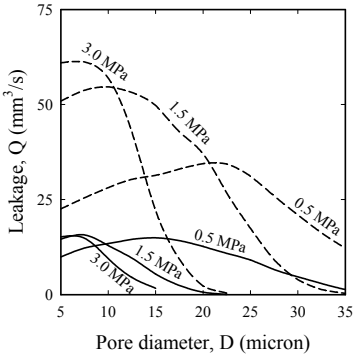


Figure 6: Effect of pore diameter on leakage rate at different sealed pressures. The solid lines are for 2.5% pore ratio and the broken lines are for 20% pore ratio.

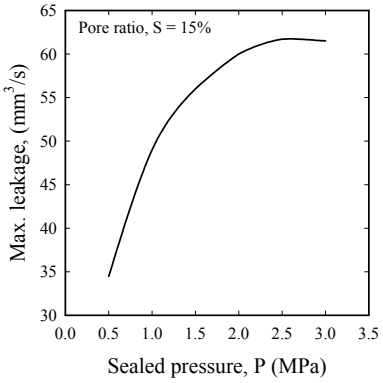


Figure 7: Effect of sealed pressures on maximum leakage rate at 15% pore ratio.

the influence of the pore diameter on the friction torque is more crucial. At small pressures, the effect of pore diameter is relatively less important. It may be noticed that at any sealed pressure, the friction torque is less at the higher pore ratio. Moreover, at higher pore ratio, the effect of the sealed pressure on the friction torque is less pronounced, which is very desirable for an application where variation in the sealed pressure is likely to be encountered.

The relationship of the minimum friction torque with pore ratio is shown in Fig. 5 for the variation of sealed pressure between 0.5 and 3 MPa. It is clearly visible that the friction torque decreases with the increase of pore ratio and thus the performance of the seal is improved. But like that with the seal clearance, the rate of improvement slows down for pore ratios beyond 15%. This is because the friction torque is closely related to the seal clearance. At a pore ratio of 15% both the seal clearance and the friction torque attain their optimum magnitudes.

Figure 6 gives the variation of the leakage flow rate with pore diameter when the sealed pressure range is from 0.5 to 3 MPa. The maximum leakage is observed at the point of the optimum pore diameter, i.e. the maximum seal clearance. Beyond the optimum pore diameter the leakage drops sharply. Below the optimum pore diameter the maximum leakage is almost insensitive of the pore diameter and the sealed pressure when the sealed pressure is large. The magnitude of leakage increases considerably

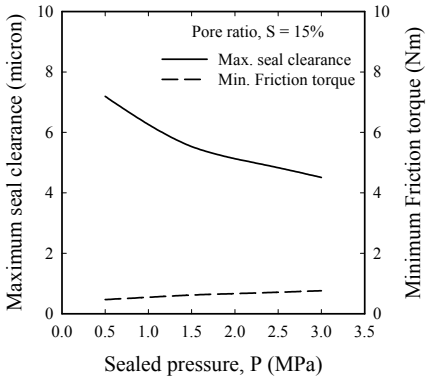


Figure 8: Effect of sealed pressures on maximum seal clearance and minimum friction torque at 15% pore ratio.

with the increase of the pore ratio, which actually indicates the necessity of a compromise between the seal clearance and the leakage when higher pore ratios are considered.

To estimate the influence of the sealed pressure on the leakage rate, the maximum leakage rates at various sealed pressures are plotted in Fig. 7 for 15% pore ratio. It is seen that the leakage increases with the increase of the sealed pressure. But for the geometry under consideration, this trend continues up to 2 MPa. Beyond this pressure, the leakage is insensitive to the sealed pressure. Figure 8 shows similar behavior also with seal clearance and friction torque.

Considering all of the performance parameters as shown in Figs. 2, 4 and 6, the optimum pore diameter appears to be 10 μm for this geomtery. At or below a pore diameter of 10 μm, the friction torque is the minimum whereas the seal clearance and hence, the leakage are the maximum. At pore diameters larger than 10 μm, the seal clearance drops and the friction torque rises very sharply. In such a case, there is a danger of seal failure through contact between the seal faces in case of a rise in sealed pressure. For a fixed pore diameter, the chance of seal failure through contact decreases with the increase of pore ratio.

## CONCLUSION

A parametric study on the performance of a non-contacting mechanical face seal with surface micropores of elliptical section has been performed using a mathematical model. It is found that better performance in terms of higher clearance and smaller friction torque can be achieved with proper selection of pore size and pore ratio. The preferable percentage of pore ratio is 15% as performance improvement becomes negligible at higher values of pore ratio. The optimum pore diameter depends on sealed pressure and pore ratio and is close to 10 μm for the geometry under consideration.

## REFERENCES

1. Salama, M. E., 1952, "The Effect of Macroroughness on the Performance of Parallel Thrust Bearings", Proc. I MechE., Vol. 163, pp. 149-158,

2. Pape, J. G.. 1968, "Fundamental Research on Radial Face Seals." ASLE Trans., Vol. 11, No. 4, pp. 302-309.

3. Etsion, I., 1980, "The Effect of Combined Coning and Waviness on the Separating Force in Mechanical Face Seals", Journal of Mech. Engg. Sci., Vol. 22, No. 2, pp. 59-64.

4. Hamilton, D. B., Walowit, J. A. and Allen, C. M., 1966, "A Theory of Lubrication by Microirregularities", Journal of Basic Engineering, Trans. ASME, Vol. 88, No. 1, pp. 177-185.

5. Anno, J. N., Walowit, J. A. and Allen, C. M., 1968, "Microasperity Lubrication.", Journal of Lubrication Technology, Trans. ASME, Vol. 91, No. 2, pp. 351-355.

6. Anno, J. N., Walowit, J. A. and Allen, C. M., 1969, "Load Support and Leakage from Microasperty Lubrication of Face Seals", Journal of Lubrication Technology, Trans. ASME, Vol. 9, No. 4, pp. 726-731.

7. Sneak, J. H., 1968, "The Effects of Geometry and Inertia on Face Seal Performance-Laminar Flow", ASME Journal of Lubrication Technology, pp. 333-340.

8. Sneak, H. J., 1968, "The Effects of Geometry and Inertia on Face Seal Performance-Turbulent Flow," ASME Journal of Lubrication Technology, pp. 342-350.

9. Lai, T. W., 1980, "Development of Non-contacting, Non-leaking Spiral Groove Liquid Face Seals", J. Lubrication Engineering, Vol. 50, No. 8, pp. 625-640.

10. Etsion, I. and Burstein, L., 1996, "Model of Mechanical Seals with Regular Micro Surface Structure", STLE Tribology Transactions, Vol. 39, No. 3, pp. 677-683.

11. Etsion, I., Halperin, G. and Greenberg, Y., 1997, "Increasing Mechanical Seals Life with Laser-Textured Mechanical Seal Faces", Proc. 15th Int. Conf. on Fluid Sealing, BHR , pp. 3-11.

12. Etsion, I., Kligerman, Y. and Halperin, G., 1999, "Analytical and Experimental Investigation of Laser-Textured Mechanical Seal Faces", STLE Tribology Transactions, Vol. 42, No. 3, pp. 511-516.

13. Faisal, M. T. R., 2006, "Effect of Pore Geometry on Face Seal Performance", Masters thesis, Dept. of Mechanical Engineering, Bangladesh University of Engineering and Technology (BUET), Dhaka-1000, Bangladesh.

14. Faisal, M. T. R. and Razzaque, M. M., 2006, "The Effects of Pore Ratio on the Performance of Mechanical Face Seals having Microirregularities in the Form of Exponential Pores", Proc. 3rd Int. Conf. on the Technological Advances of Thin Films and Surface Coatings - THINFILMS 2006, Grand Copthrone Waterfront Hotel, Singapore, pp. 304-305.